NASA TECHNICAL NOTE

NASA TN D-4387

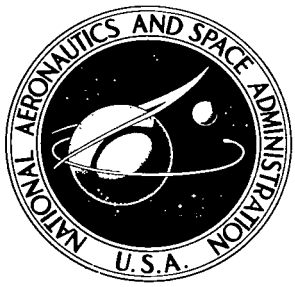

NASA TN D-4387

VENTURI SCALING STUDIES ON THERMODYNAMIC EFFECTS OF DEVELOPED CAVITATION OF FREON-114

by Royce D. Moore and Robert S. Ruggeri

Lewis Research Center
Cleveland, Ohio

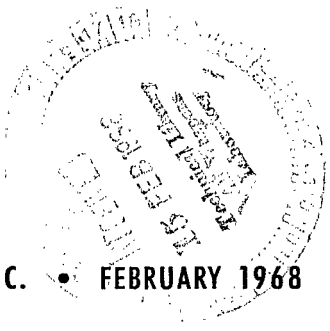

NATIONAL AERONAUTICS AND SPACE ADMINISTRATION • WASHINGTON, D. C. • FEBRUARY 1968

VENTURI SCALING STUDIES ON THERMODYNAMIC EFFECTS OF DEVELOPED CAVITATION OF FREON-114

By Royce D. Moore and Robert S. Ruggeri

Lewis Research Center
Cleveland, Ohio

NATIONAL AERONAUTICS AND SPACE ADMINISTRATION

For sale by the Clearinghouse for Federal Scientific and Technical Information
Springfield, Virginia 22151 – CFSTI price $3.00

CONTENTS

VENTURI SCALING STUDIES ON THERMODYNAMIC EFFECTS OF DEVELOPED CAVITATION OF FREON-114

by Royce D. Moore and Robert S. Ruggeri

Lewis Research Center

SUMMARY

Well-developed cavitation of Freon-114 (dichlorotetrafluorethane) was induced on the walls of a venturi in a recirculating hydrodynamic tunnel. The venturi, which had a throat diameter of 0.976 inch (2.48 cm), was a 0.7 scale of one previously tested. The approach velocity was varied from 20 to 50 feet per second (6.1 to 15.2 m/sec) at controlled liquid temperatures from 0° to 86° F (255.4° to 303.2° K). Pressures and temperatures were measured in the cavitated region and compared with the results of the 1.0-scale venturi. For geometrically similar cavities and fixed flow velocity, the measured cavity pressure and temperature depressions below free-stream values of vapor pressure and temperature were nearly the same for both the 0.7- and 1.0-scale venturis. Cavity pressure and temperature depression trends with liquid temperature and velocity were also similar in the 0.7-scale venturi as in the 1.0-scale venturi. A previously derived method for predicting the thermodynamic effects of cavitation is extended to include the effect of scale. Similarity parameters for developed cavitation were evaluated by using the minimum cavity pressure as a reference rather than the free-stream vapor pressure. The cavitation parameter was shown to be nearly the same value for both the 0.7- and 1.0-scaled venturis.

INTRODUCTION

The high-performance propellant pumps used in rocket engines generally employ an inducer stage ahead of the main rotor. The inducer is capable of operating with cavitation present on the suction surface of the blades. However, the physical properties of the liquid being pumped have pronounced effects on the cavitation performance. A pump operated under cavitating conditions in liquid hydrogen, butane, methyl alcohol, Freon, and hot water, for example, will have better cavitation performance (lower net positive

suction head (NPSH) requirements) than when operated in cold water (refs. 1 to 5). This improvement in cavitation performance has been attributed to the thermodynamic effects of cavitation resulting from the varying degrees of evaporative cooling. This cooling lowers the vapor pressure in the cavity which then lowers, by the same amount, the NPSH requirements for a given performance level.

In order to determine the magnitude of these thermodynamic effects of cavitation, it is necessary to measure the pressures and temperatures within the cavitated region. To simplify the instrumentation and for easier study, nonrotating flow devices such as venturis can be used to learn more about flow conditions in pumps. Cavitation studies in a venturi (refs. 6 and 7), in which pressures and temperatures within cavitated regions were measured directly, show that the thermodynamic effects of cavitation can be predicted for a given venturi for a range of flow velocity, liquid, or liquid temperature. This prediction method requires measurement of cavity pressure at one operating point. The prediction method determined from the venturi studies has been successfully applied in reference 2 to the prediction of pump cavitation performance. Reference values of cavitation performance must be established from experiment for the pump of interest.

Because of the cost of facilities and propellants to test the large full-scale propellant pumps, it would be desirable to use more economical test procedures such as scale models, reduced speed, or inexpensive test fluids in order to predict the cavitation performance of the large propellant pumps. As previously indicated, the prediction method of reference 2 accounts for speed and liquid variations, but does not account for scale effects.

The purpose of this investigation was to evaluate the effect of scale on the thermodynamic effects of cavitation. A 0.7-scale model of the venturi used in previous studies (refs. 6 to 10) was used as the test section. Pressures and temperatures were measured within cavitated regions and these measurements were compared with the results obtained for the full-size venturi. The previously derived prediction method of reference 6 is extended to include the effect of scale on the thermodynamic effects of cavitation. Freon-114 (dichlorotetrafluoroethane) was used as the test fluid. The 0.7-scaled venturi had a 0.976-inch (2.48-cm) diameter throat. The flow velocity in the venturi approach section was varied from 20 to 50 feet per second (6.1 to 15.2 m/sec) at controlled temperatures from 0° to 86° F (255.4° to 303.2° K). The study was conducted at NASA Lewis Research Center.

APPARATUS

Facility

The facility used in the present study is the same as that described in detail in ref-

erences 7 and 10. Briefly, it consists of a small recirculating hydrodynamic tunnel with a capacity of 10 gallons (37.85 liters). The tunnel was designed to circulate various liquids by means of a centrifugal pump. Static-pressure level in the tunnel was varied by gas pressurization of the ullage space above a butyl rubber diaphragm in the tunnel expansion chamber. The entire tunnel loop was submerged in a bath of ethylene glycol - water mixture which was used to control tunnel liquid temperature. This bath mixture exchanged heat with a sump-mounted, single-tube coil, which carried either low-pressure steam or cold nitrogen gas.

Venturi Test Section

The transparent-plastic venturi test section (fig. 1) is a 0.7-scale model of the one

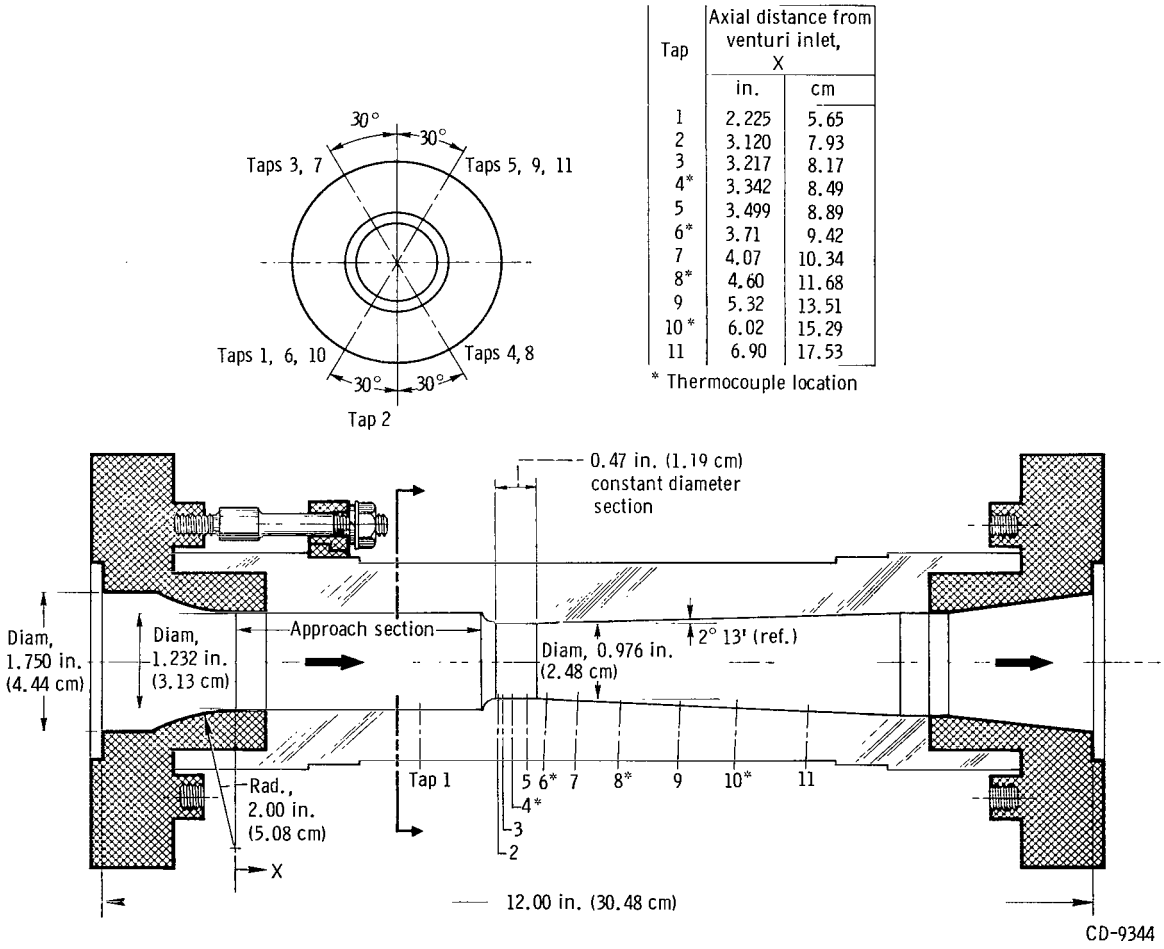

Tap	Axial distance from venturi inlet, X	
	in.	cm
1	2.225	5.65
2	3.120	7.93
3	3.217	8.17
4*	3.342	8.49
5	3.499	8.89
6*	3.71	9.42
7	4.07	10.34
8*	4.60	11.68
9	5.32	13.51
10*	6.02	15.29
11	6.90	17.53

* Thermocouple location

Figure 1. - Schematic drawing of venturi test section.

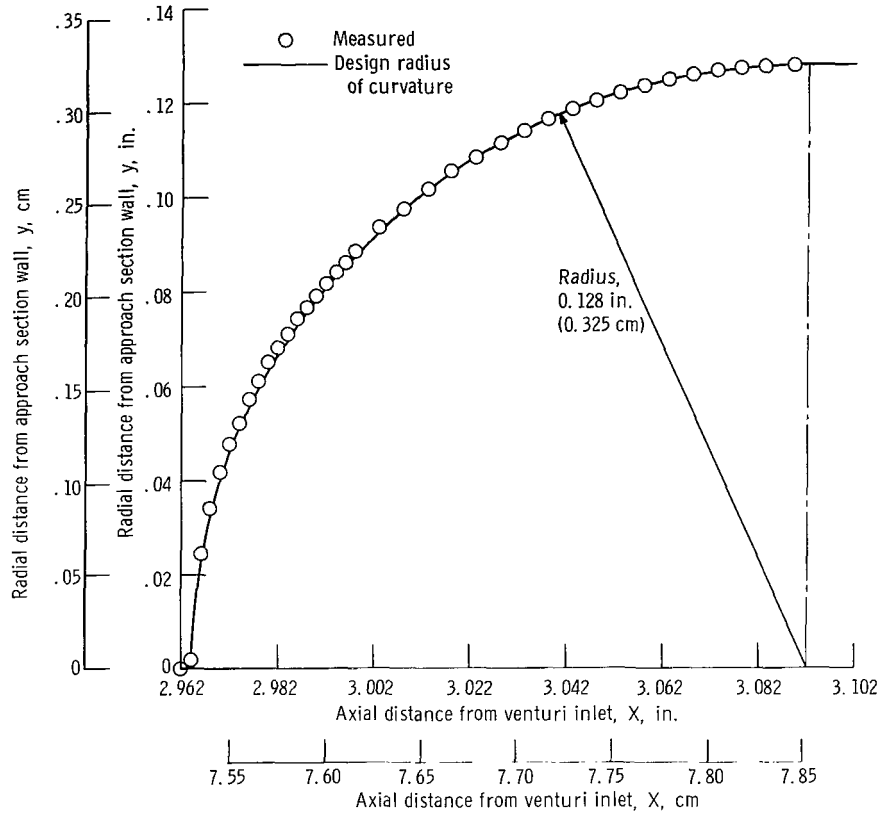

Figure 2. - Contour of quarter-round section of 0.7 scale venturi.

used in previous cavitation studies (refs. 6 to 10). The venturi incorporates a quarter-round to provide the transition from the approach section to a constant-diameter throat section. A comparison of the finished contour and the design radius of curvature of the quarter-round section is presented in figure 2.

The venturi used in the present study will be called the 0.7-scale venturi. The venturi of references 6 to 10 will be called the 1.0-scale venturi.

A greater difference in scale would have been desirable, but the flow capacity of the facility and instrumentation size limited the scale factor to 0.7. The 0.7-diameter ratio, however, results in one-half the flow area of the 1.0-scale venturi.

Instrumentation

For velocity determination, static pressures were measured across the tunnel contraction nozzle (not shown herein, see ref. 10) just upstream of the test section. This

velocity was then corrected using continuity for flow area changes between nozzle exit and approach section. Contraction nozzle pressures and those from tap 1 in figure 1 were measured by calibrated precision gauges (accuracy, ±0.15 psi (±0.1 N/cm^2)). The six pressure taps, used to measure pressures within the cavity, were connected to a 4-foot-high (1.2 m) multiple-tube mercury manometer. All pressure lines were arranged in a horizontal plane on the venturi centerline before leaving the tunnel bath wall to minimize hydrostatic head corrections.

The liquid temperature was measured by means of a calibrated copper-constantan thermocouple mounted on the tunnel centerline approximately 14.5 inches (36.83 cm) upstream of tap 1. Four thermocouples were mounted to coincide with the venturi wall contour, but they did not contact the wall. The calibrated copper-constantan thermocouple circuit was designed to measure the temperature difference between a venturi innerwall location and the upstream liquid reference. The temperature differences were measured with an accuracy of ±0.05° F (±0.03° K) and tunnel liquid temperature level with an accuracy of ±0.2° F (±0.1° K).

Cavitation was photographed by a 4- by 5-inch (10.2- by 12.7-cm) still camera with a 0.5-microsecond high-intensity flash unit.

PROCEDURE

Test Liquid

A commercial grade of Freon-114 was used as the test liquid. It is a clear, colorless liquid with a normal boiling point of 38.8° F (277.0° K). The physical properties of Freon-114 used herein were obtained from references 11 to 13.

The tunnel was evacuated and cooled to below 38° F (276.5° K) before filling with Freon-114. Freon-114 was transferred directly to the tunnel from the shipping cylinder. The manufacturer specifies a noncondensable gas content (assumed to be air) less than 20 parts per million (mg air/kg liquid). Air-saturated Freon-114 at a total pressure of 1 atmosphere (10.1 N/cm^2) contains about 140 parts per million at 32° F (273.2° K) and about 1000 parts per million at 0° F (255.4° K).

Facility Operation and Measurement Techniques

To minimize air contamination of the tunnel liquid, all pressure lines and manometer tubes were evacuated before the tunnel was filled. The valves between the venturi and manometer were closed after this evacuation. For the pressure measurements within a

cavitated region, a manometer tube was opened only after cavitation was developed over the corresponding pressure tap. Downstream taps were similarly activated as the cavity length was increased. In this way, no liquid Freon-114 was permitted to reach the manometer tubes; therefore, no hydrostatic head corrections to the manometer readings were needed.

At the desired pump speed and tunnel liquid temperature, the free-stream static pressure was decreased to form a cavity of nominally fixed length. Pressures and temperatures within the cavitated region were then measured. The tunnel liquid temperature varied less than $\pm 0.2^{\circ}$ F ($\pm 0.1^{\circ}$ K) for a given test point. Four different cavity lengths were generated at each of the several pump speeds and liquid temperatures. Nominal cavity lengths of 0.3, 0.7, 1.6, and 3.0 inches (0.8, 1.8, 4.1, and 7.6 cm) were selected because they approximate 0.7 the cavity lengths used in the 1.0-scale venturi studies (ref. 6). Each successive increase in cavity length allowed additional pressure tap and thermocouple locations to be included within the cavity. For a fixed pump speed, the free-stream velocity decreased with increased cavity length because of increased total head losses.

RESULTS AND DISCUSSION

The experimental Freon-114 results in the 0.7-scale venturi are presented first, followed by a comparison of the experimental results for both the 0.7- and 1.0-scale venturis. Finally, experimental results are compared with a prediction method which is extended herein to include the effect of scale on the thermodynamic effects of cavitation.

Results from 0.7-Scale Venturi Tests

Wall pressure distribution. - The 0.7-scale venturi incorporates an essentially true circular arc as a convergence section, whereas the previously studied 1.0-scale venturi contained a slightly modified circular arc. Because the thermodynamic effects of cavitation were shown in reference 11 to be, in some manner, dependent on the wall pressure distribtuion and because wall pressure distribution is, in turn, dependent on wall contour, the pressure distribution was experimentally determined for both the 0.7-scale venturi (true quarter round) and the 1.0-scale venturi (modified quarter round). The pressure distributions were not measurably different. The pressure coefficient C_p for the 0.7-scale venturi is plotted in figure 3 as a function of axial distance from the minimum pressure location. The data were obtained from both hydrodynamic measurements using Freon-114 and from aerodynamic studies with a 6.5-scale model, which was large enough

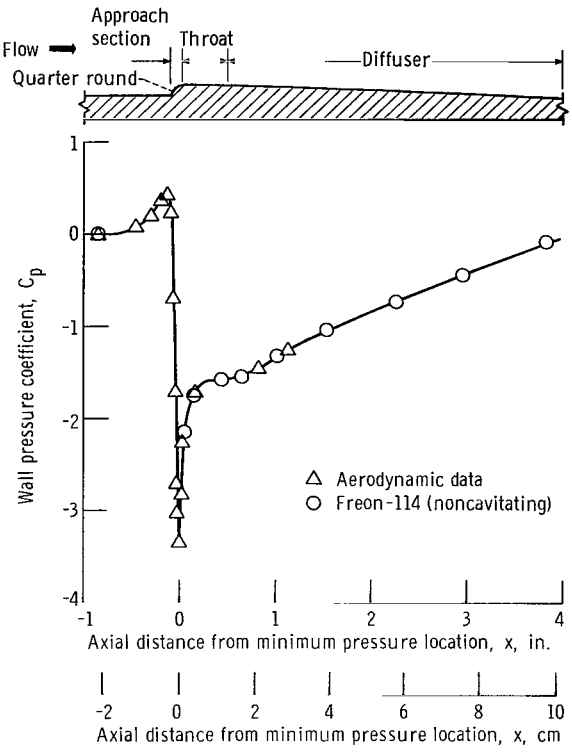

Figure 3. - Wall pressure distribution for the 0.7-scale venturi. Minimum pressure location at axial distance from venturi inlet, 3.065 inch (7.79 cm).

to incorporate several pressure taps on the quarter-round section. These aerodynamic data had been previously obtained in support of the venturi studies of references 6 to 10.

Appearance of developed cavitation. - Photographs of typical 0.7- and 1.6-inch (1.8- and 4.1-cm) cavities are shown in figure 4. For the range of conditions studied, a change in free-stream temperature or velocity did not change the appearance of fixed-length Freon-114 cavitation. The cavitation is composed of many individual vapor streamers around the periphery of the venturi that merge within a few tenths of an inch downstream from the leading edge of the cavity to form a thin annulus of frothy and turbulent vapor-droplet mixture adjacent to the wall. The leading edges of these streamers remained fixed at or near the minimum pressure location. Within the venturi throat, the nominal thickness of the cavitated region is estimated to be between 0.01 and 0.03 inch (0.03 to 0.08 cm) although no direct measurements were made. Thus, a large part of the flow remains single phase (liquid) in the central portion of the venturi under all conditions of cavitation studied.

Typical cavity pressure and temperature distribution. - Within the cavitated regions, local pressures and temperatures are less than free-stream values of vapor pressure

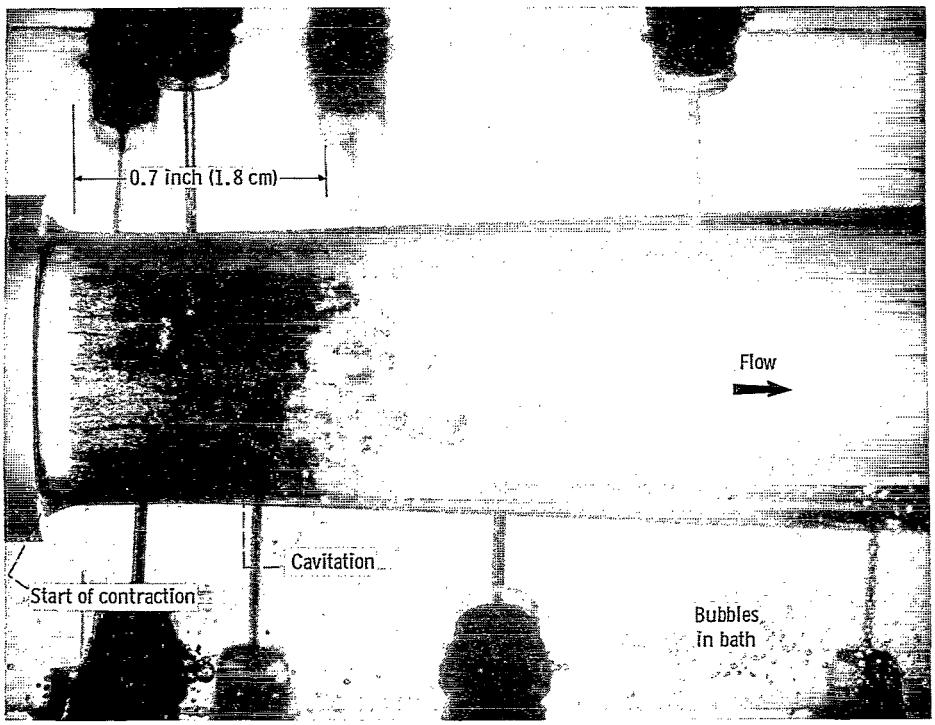

(a) Cavity length, 0.7 inch (1.8 cm).

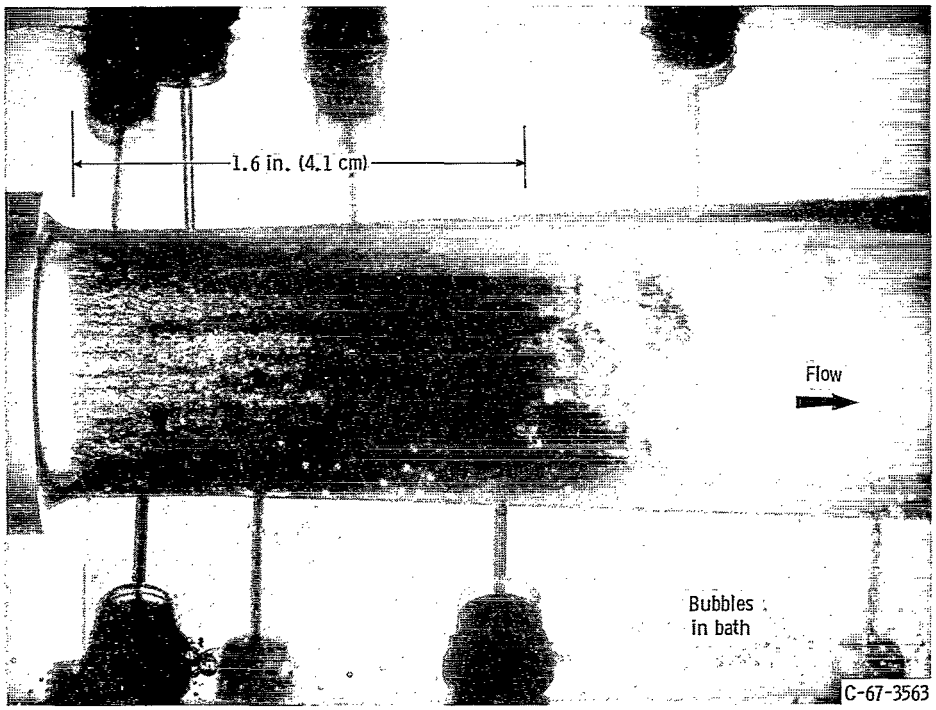

(b) Cavity length, 1.6 inches (4.1 cm).

Figure 4. - Typical cavitation for Freon-114 in 0.7-scale venturi.

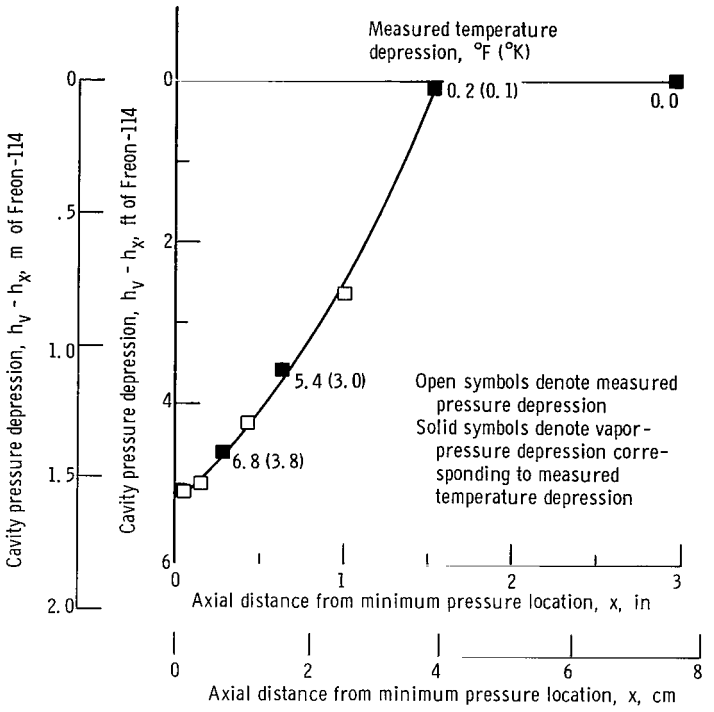

Figure 5. - Typical pressure and temperature depressions within cavitated Freon-114 region. Nominal cavity length, 1.6 inches (4.1 cm); free-stream velocity, 31.1 feet per second (9.5 m/sec); free-stream static pressure, 66.4 feet (20.2 m); liquid temperature, 60.7° F (289.1° K).

and temperature. Typical results for a 1.6-inch (4.1-cm) cavity are given in figure 5. Cavity pressure depressions are presented as a function of axial distance from the minimum pressure location. The measured pressure depressions (open symbols) are relative to free-stream vapor pressure. The measured temperature depressions (numbers along curve) were converted to the corresponding vapor-pressure depression (solid symbols) by using the vapor pressure-temperature curve obtainable from reference 12. The good agreement between the measured pressure depressions and the depressions based on locally measured temperatures indicates, that for the accuracy required for engineering purposes, the pressures and temperatures within the cavity are in thermodynamic equilibrium.

The maximum measured pressure depressions occur near the leading edge of the cavitated region. The pressure and temperature depressions approach zero near the observed end of the cavitated region. Downstream from the collapse region, the liquid along the wall returns to the free-stream temperature. The absolute value of wall pressure downstream from the cavity increases and approaches the noncavitating value shown in figure 3 except for the energy losses due to mixing.

Cavitation similarity parameters. - The conventional cavitation parameter is usually expressed as

$$K_v \equiv \frac{h_0 - h_v}{\frac{V_0^2}{2g}} \tag{1}$$

The parameter K_v for developed cavitation is derived from the assumption that

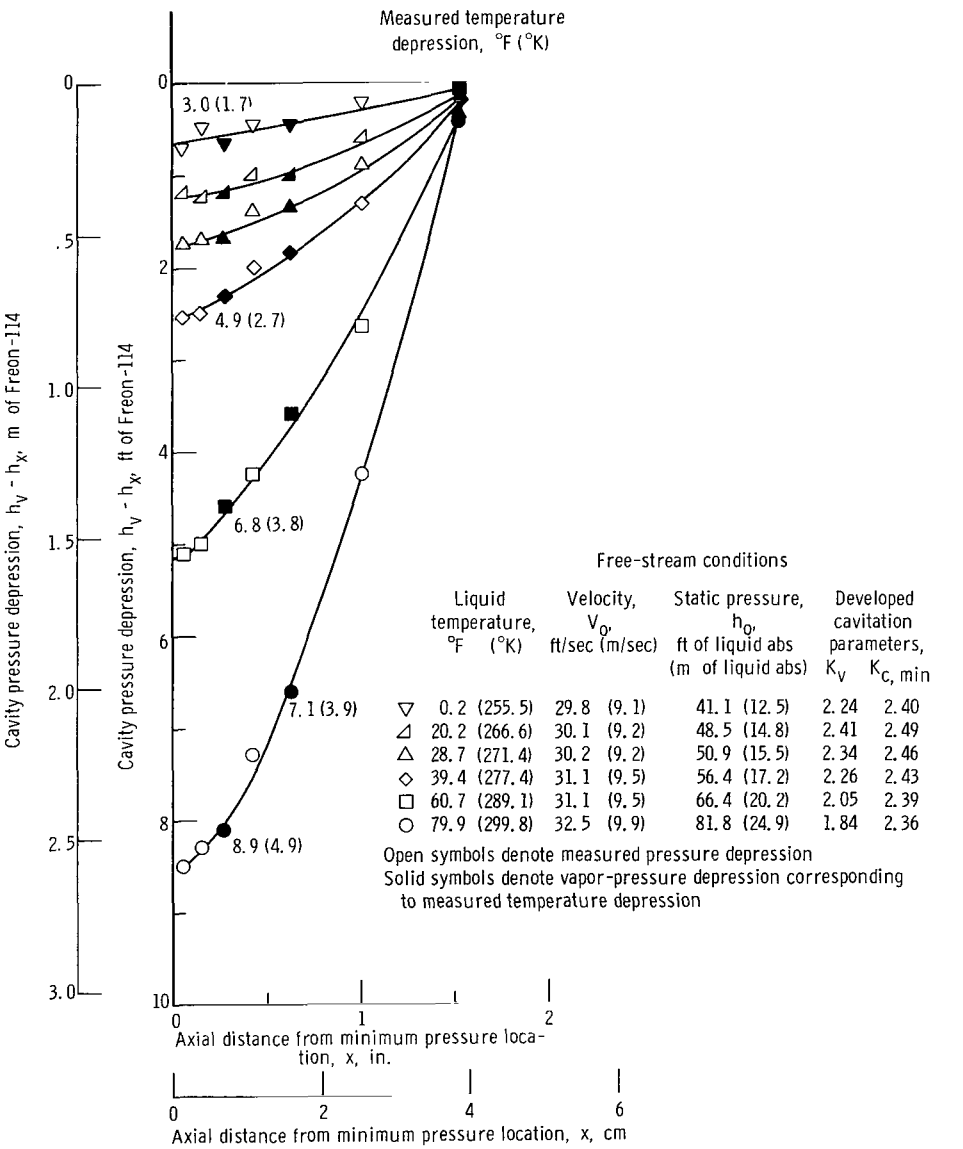

Figure 6. - Effect of free-stream liquid temperature on pressure and temperature depressions within cavitated Freon-114 region for cavity length of 1.6 inches (4.1 cm).

Bernoulli's equation for steady ideal flow applies between a free-stream location and the cavity surface and that the cavity surface is at a constant pressure equal to free-stream vapor pressure. A more general expression for the cavitation parameter would replace h_v in equation (1) with h_c, the actual pressure in the cavity. The pressure within the cavitated region of Freon-114 is less than the free-stream vapor pressure and varies with axial distance as shown in figure 5 so that a selection of a reference cavity pressure is required. The minimum measured cavity pressure (corresponding to maximum cavity pressure depression) is used herein as well as in reference 6 to define a developed cavitation parameter.

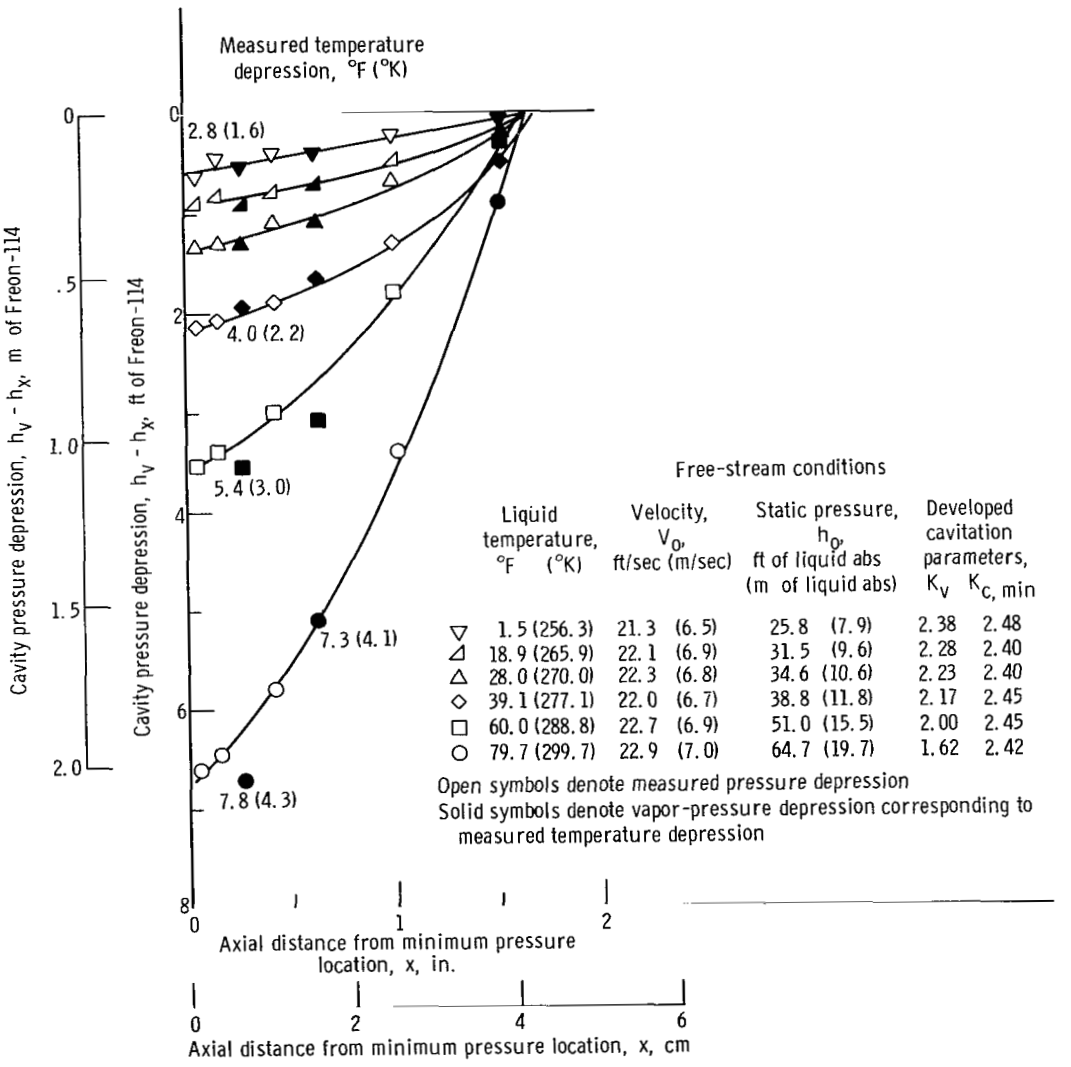

(a) Nominal free-stream velocity, 22.2 feet per second (6.7 m/sec).

Figure 7. - Effect of free-stream velocity on pressure and temperature depressions within cavitated Freon-114 region at several liquid temperatures for cavity length of 1.6 inches (4.1 cm).

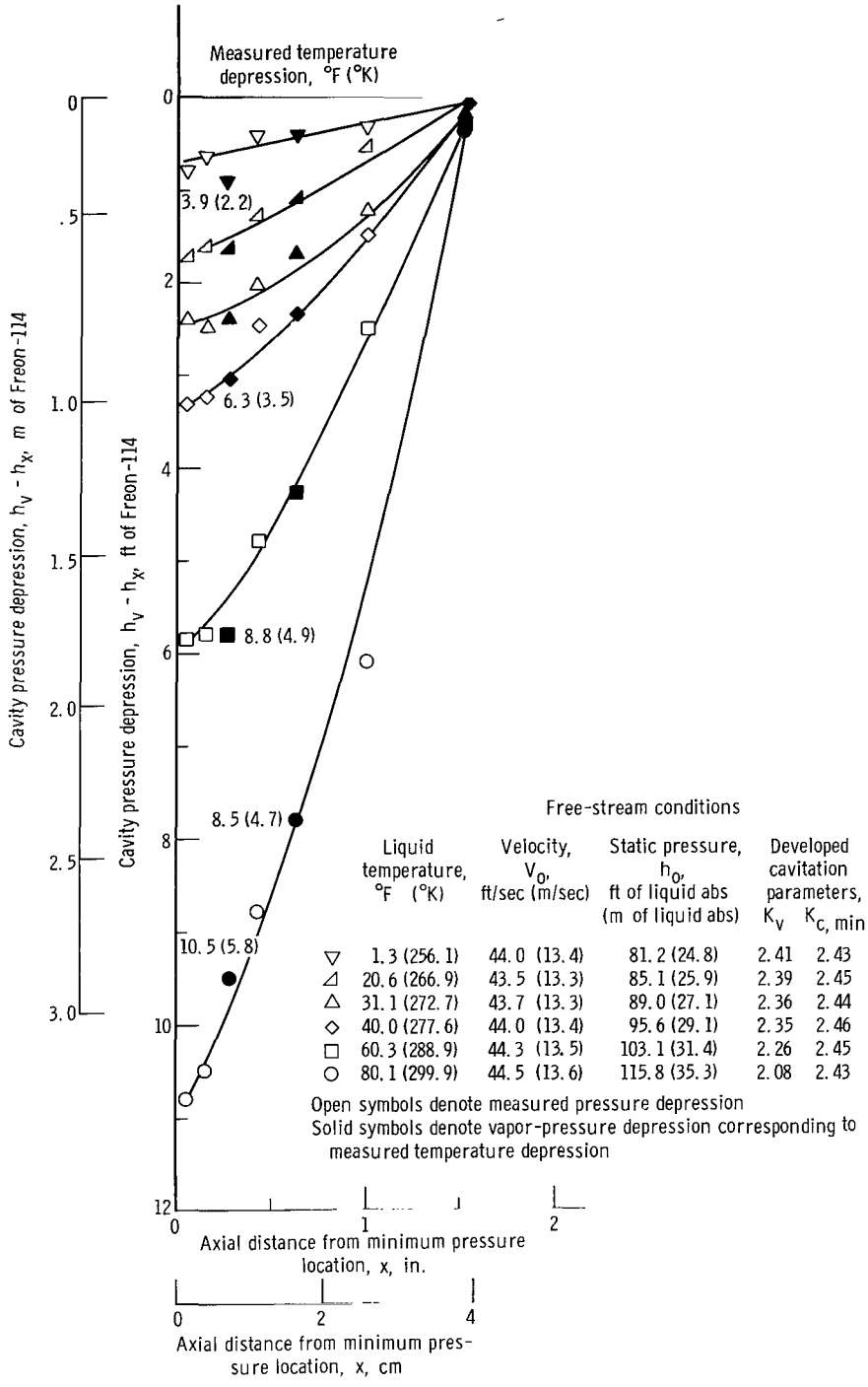

(b) Nominal free-stream velocity, 44.0 feet per second (13.4 m/sec)

Figure 7. - Concluded.

$$K_{c,\,min} \equiv \frac{h_0 - h_{c,\,min}}{\frac{V_0^2}{2g}} = \frac{h_0 - h_v + (h_v - h_{c,\,min})}{\frac{V_0^2}{2g}} = K_v + \frac{(\Delta h_v)_{max}}{\frac{V_0^2}{2g}} \qquad (2a)$$

The maximum cavity pressure depression was selected because, as shown in reference 6, a change in $(\Delta h_v)_{max}$ results in a corresponding change in free-stream static pressure h_0. Therefore, the value of $K_{c,\,min}$ is nearly constant over a range of velocities and

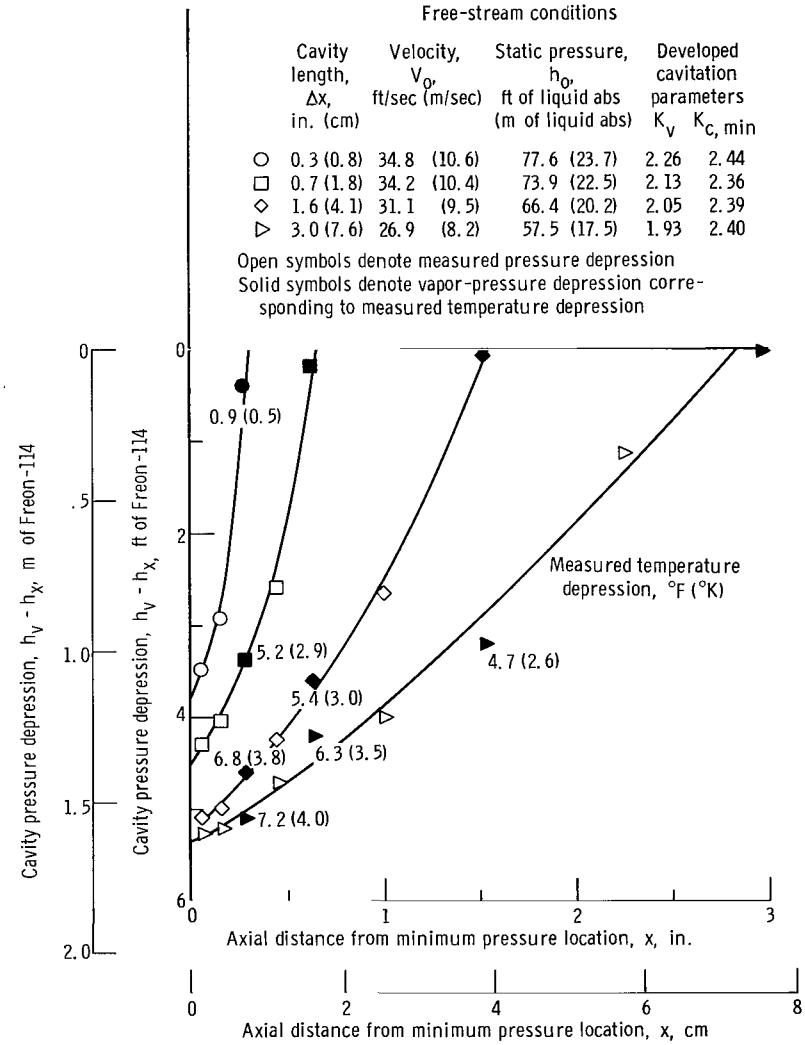

Figure 8. - Effect of cavity length on pressure and temperature depressions within cavitated Freon-114 regions for free-stream liquid temperature of 60.7° F (289.1° K).

temperatures, whereas K_v (eq. (1)) varies considerably and is therefore less useful as a similarity parameter.

Specific trends in cavity pressure depression. - The measured values of cavity pressure (and temperature) depressions for the 0.7-scale venturi are shown in figures 6 to 8. The trends observed with variation in free-stream temperature, velocity, and cavity length are very similar to those obtained with the 1.0-scale venturi.

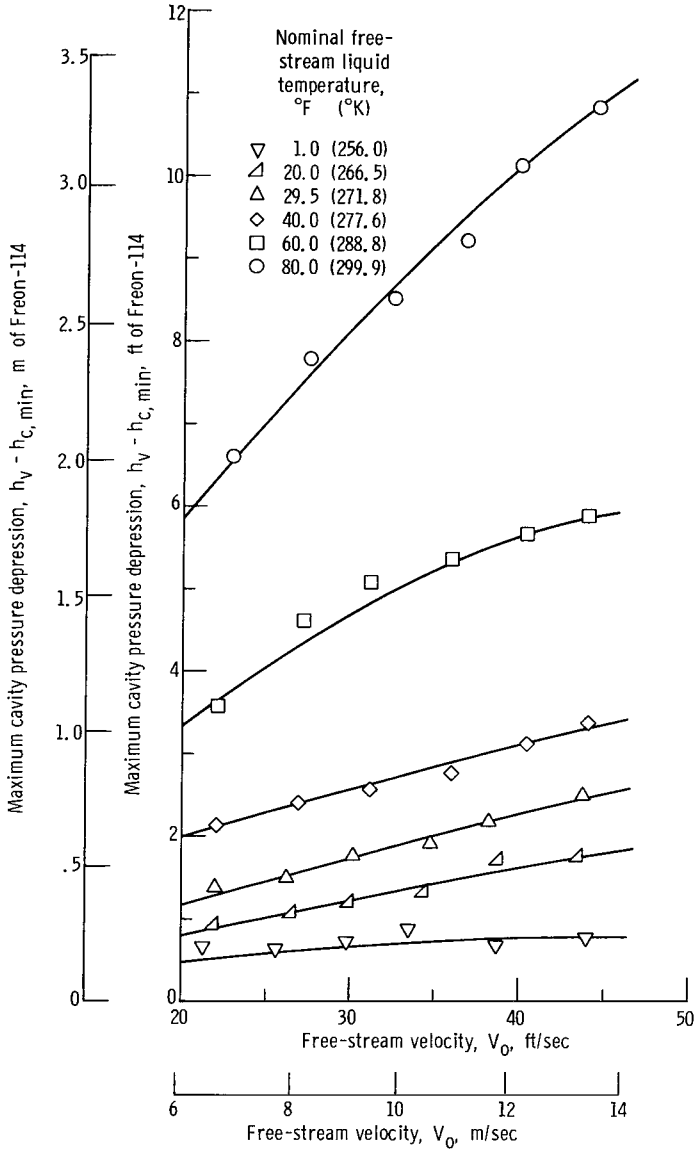

Figure 9. - Effects of free-stream velocity and liquid temperature on maximum pressure depression within cavitated Freon-114 region for cavity length of 1.6 inches (4.1 cm).

The depression in cavity pressure (and temperature) over the full axial length of the cavity increases at higher temperature (fig. 6). A proportionally greater increase in cavity pressure depression is observed at the higher temperatures.

Increasing the free-stream velocity by a factor of 2 results in nearly a twofold increase in the cavity pressure depression (fig. 7(b) as compared with fig. 7(a)). Similar trends occur for the five temperature levels shown.

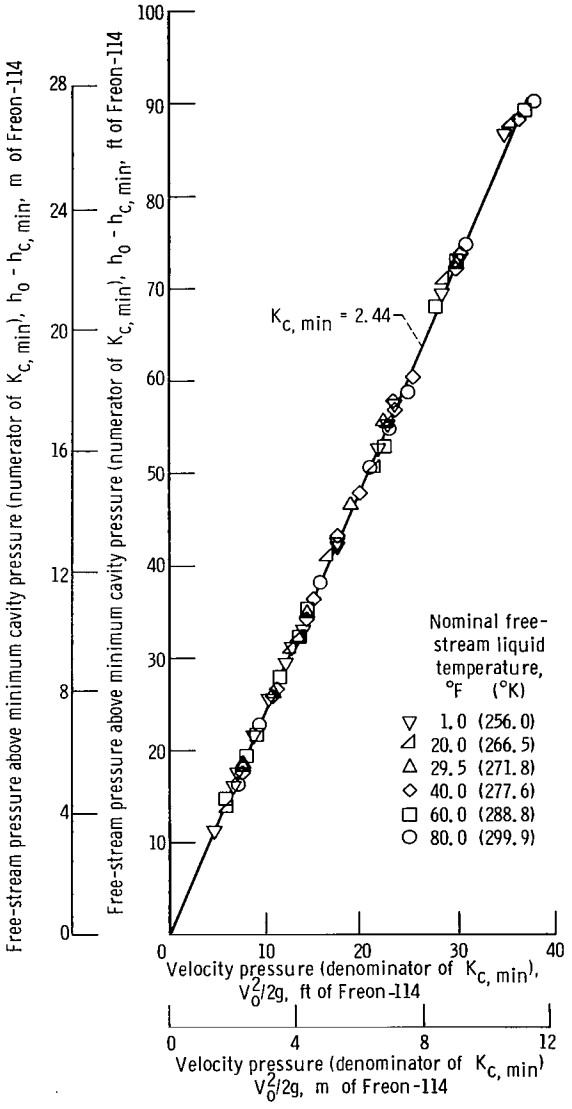

Figure 10. - Effects of free-stream velocity and liquid temperature on minimum pressure in cavitated Freon-114 region. Cavity length, 0.3 to 3.0 inches (0.8 to 7.6 cm).

As the cavity length was increased, the cavity pressure (and temperature) depressions increased over the full axial length of the cavity, as shown in figure 8.

The maximum pressure depressions, which are used to determine $K_{c,min}$ are summarized for 1.6-inch (4.1-cm) cavities over a range of velocities and temperatures in figure 9. The maximum measured pressure depressions increase almost directly with increasing velocity at constant temperature. The cavity pressure depressions increase continuously with increasing temperature at constant velocity. Similar results were obtained for the other cavity lengths.

The cavitation parameter $K_{c,min}$, tabulated for all the data on figures 6 to 8, remains nearly constant. Although the data represent a range of velocities, temperatures, and cavity lengths, $K_{c,min}$ varies in a random manner between 2.36 and 2.49. In contrast, K_v has noticeable trends with velocity, temperature, and cavity length. And it decreases with increasing temperature and increasing cavity length and increases with increasing velocity.

The degree to which $K_{c,min}$ is constant is shown graphically in figure 10, where the numerator of $K_{c,min}$ is plotted as a function of its denominator. The line shown is for a $K_{c,min}$ of 2.44 and the close agreement with the data indicates that this single value can be utilized to represent all the data. This value is independent of free-stream liquid temperature and velocity, and, for this venturi, it is independent of cavity length.

Effect of Venturi Scale on Cavity Pressure Depressions

A comparison of the cavity pressure depression effects for the 0.7- and 1.0-scale venturis is presented in figure 11, where the cavity pressure depression is plotted as a function of the ratio of axial distance to free-stream diameter. The data are for a cavity length corresponding to a $\Delta x/D$ of 1.4 and are typical for all $\Delta x/D$-values studied. For a nominal velocity of 31 feet per second (9.4 m/sec), the cavity pressure depressions are nearly the same for both models over the entire length of the cavity. The same trend is present for each of the three temperatures shown.

The cavitation parameter $K_{c,min}$ is nearly constant for both venturis and independent of temperature. Although K_v is constant for both venturis at each temperature, K_v decreases with increasing temperature.

For each temperature, the free-stream static pressure, h_0 (tabulated on fig. 11) is essentially independent of scale. Because h_0 and the pressures within the cavitated region are nearly the same for each temperature, the geometric flow conditions for the 0.7-scale venturi must be similar to those for the 1.0-scale venturi for a fixed value of $\Delta x/D$.

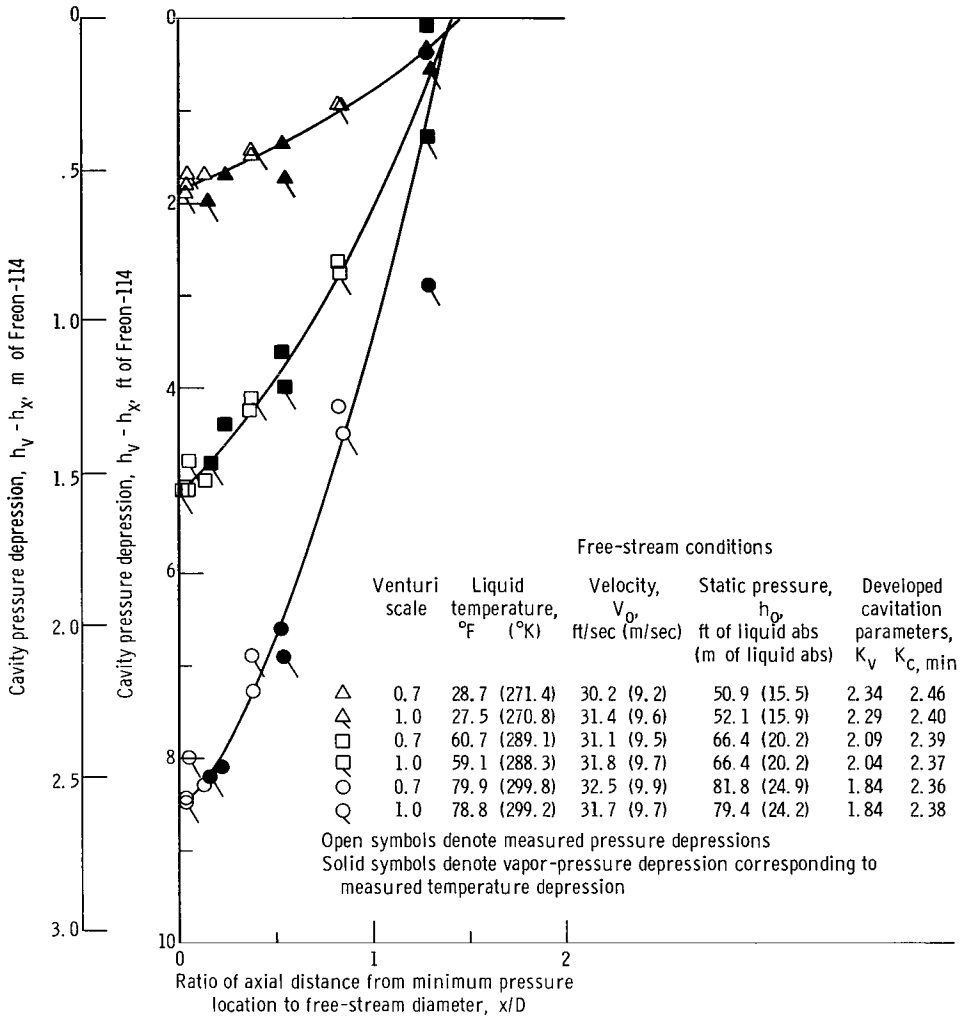

Figure 11. - Effect of venturi scale on pressure and temperature depressions within cavitated Freon-114 regions for nominal cavity length of 1.4 free-stream diameters.

The effect of venturi scale on the maximum cavity pressure depression is presented in figure 12 where the maximum measured cavity pressure depression is shown as a function of free-stream velocity and liquid temperature. The nominal cavity length is 1.4 free-stream diameters. For the two scaled venturis, the maximum cavity pressure depression is essentially independent of scale for fixed $\Delta x/D$ over the ranges of velocity and temperature tested.

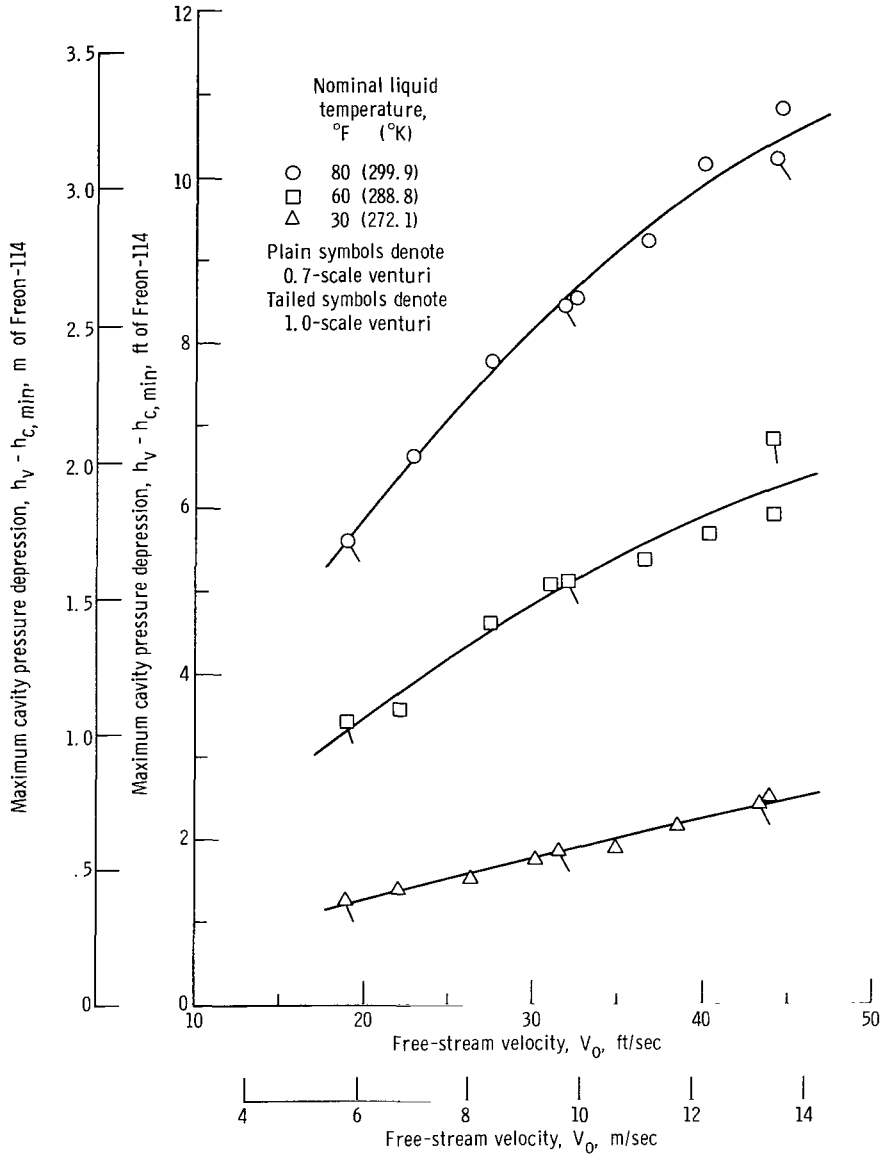

Figure 12. - Effect of venturi scale on maximum cavity pressure depression for Freon-114. Nominal cavity length of 1.4 free-stream diameters.

Analytical Considerations

Heat balance. - The temperature depressions measured within a cavitated region are attributed to liquid cooling along the vapor-liquid interface because of the heat of vaporization drawn from a thin layer of adjacent liquid. If the conditions within the cavity are in thermodynamic equilibrium (and there are no partial pressures of permanent gases), the cavity pressure should drop to the vapor pressure corresponding to the reduced local temperature. The vapor pressure depression is a function of the physical properties of the fluid, body geometry, velocity, and the heat and mass transfer mechanisms involved. The magnitude of the vapor pressure depression can be estimated by setting up a heat balance between the heat required for vaporization and the heat drawn from the surrounding liquid. From this heat balance, it can be shown that a useful approximation of the vapor pressure depression is

$$\Delta h_v \cong J \left(\frac{\rho_v}{\rho_l}\right)^2 \left(\frac{L^2}{C_l T}\right)\left(\frac{\mathcal{V}_v}{\mathcal{V}_l}\right) \tag{3}$$

The derivation of the vapor pressure depression is given in reference 6. All the terms in equation (3) are fluid properties and are known except the vapor- to liquid-volume ratio $\mathcal{V}_v/\mathcal{V}_l$. In the experimental case the absolute value of volume ratio cannot be directly determined because $\mathcal{V}_l$ is only that volume of liquid actually involved in the vaporization process. Thus, $\mathcal{V}_l$ is only a fraction of the entire liquid stream. However, Δh_v can be expressed as a function of $\mathcal{V}_v/\mathcal{V}_l$ for any liquid whose fluid properties are known, and this is done for Freon-114 and liquid nitrogen in figure 13. (This figure is repeated from ref. 6.) With figure 13, useful predictions are possible by obtaining a reference value of $\mathcal{V}_v/\mathcal{V}_l$ from measured cavity pressure depressions for one model scale, liquid, temperature, and velocity and then estimating relative values of $\mathcal{V}_v/\mathcal{V}_l$ for other liquids, temperatures, velocities, and model scales. With these latter values of $\mathcal{V}_v/\mathcal{V}_l$, the values of Δh_v at the conditions of interest can be determined. A method for estimating values of $\mathcal{V}_v/\mathcal{V}_l$ from a known reference value is developed in the following section.

Geometric scale effects on volume ratio. - The vapor volume is assumed to be proportional to the product of cavity length, model diameter, and average cavity thickness ($\mathcal{V}_v \sim \Delta x D \delta_v$). Liquid volume is assumed proportional to the product of cavity length, model diameter, and the average thickness of the liquid element supplying the heat for vaporization ($\mathcal{V}_l \sim \Delta x D \delta_l$). In a given model the vapor- to liquid-volume ratio $\mathcal{V}_v/\mathcal{V}_l$ is therefore proportional to δ_v/δ_l. Thus, the volume ratio for the scale model can be expressed as,

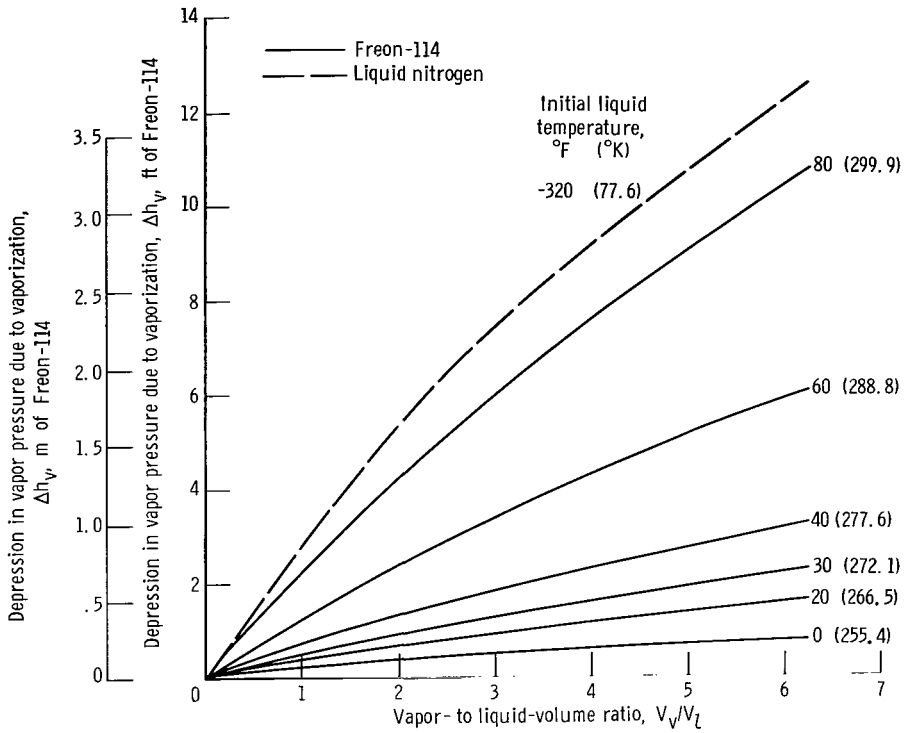

Figure 13. - Vapor pressure depression as function of amount of liquid vaporized for several temperatures for Freon-114 and liquid nitrogen.

$$\left(\frac{\rho_v}{\rho_l}\right)_s = \frac{\left(\frac{\rho_v}{\rho_l}\right)_f \left(\frac{\delta_v}{\delta_l}\right)_s}{\left(\frac{\delta_v}{\delta_l}\right)_f}$$

The following analyses for determination of the volume ratio for a scaled model relative to that for a full-size model will be made on the basis of the same scaled cavity length; that is, $\Delta x/D$ is the same for both models. As previously discussed, a scaled cavity length provides geometrically similar flow conditions in both venturis. Thus, the cavity thickness and cavity length will vary directly with scale factor, that is,

$$\frac{\delta_{vs}}{\delta_{vf}} = \frac{D_s}{D_f} \quad \text{and} \quad \frac{\Delta x_s}{\Delta x_f} = \frac{D_s}{D_f} \tag{4}$$

Various theoretical analyses have shown that the liquid layer thickness is proportional to the product of thermal diffusivity and vaporization to some power, $\left[\delta_l \sim (\alpha\tau)^Z\right]$, where $0 < z \leq 1$. The exponent z depends on the heat-transfer process involved. In a previous investigation (ref. 6), it was shown that the exponent z, determined experimentally, was not the same for α and τ; therefore the exponent for α and for τ will be separately evaluated. With τ proportional to $\Delta x/V_0$, δ_l is proportional to $\alpha^m(\Delta x/V_0)^n$. The volume ratio $(\forall_v/\forall_l)_s$ for the scaled model can thus be expressed as

$$\left(\frac{\forall_v}{\forall_l}\right)_s = \left(\frac{\forall_v}{\forall_l}\right)_f \left(\frac{\delta_{v,s}}{\delta_{v,f}}\right) \left(\frac{\alpha_f}{\alpha_s}\right)^m \left(\frac{\Delta x_f}{\Delta x_s}\right)^n \left(\frac{V_{0,s}}{V_{0,f}}\right)^n$$

Expressing the cavity thickness ratio and the cavity length ratio in terms of the diameter ratio (eq. (4)), the volume ratio becomes

$$\left(\frac{\forall_v}{\forall_l}\right)_s = \left(\frac{\forall_v}{\forall_l}\right)_f \left(\frac{\alpha_f}{\alpha_s}\right)^m \left(\frac{D_s}{D_f}\right)^{1-n} \left(\frac{V_{0,s}}{V_{0.f}}\right)^n \tag{5}$$

Experimental Freon-114 data from both the 0.7- and 1.0-scale venturis are used to evaluate the exponents m and n in equation (5). Cavity pressure depression data are available for conditions in which only α was varied, while V_0 and D were held constant. From these data and the theoretical relation between Δh_v and $\forall_v/\forall_l$ (fig. 13), the exponent m on the α-ratio term can be determined. In a similar manner in which V_0 is the only variable, the exponent n can be determined. The exponent for the diameter ratio term presently comes via theory from the exponent n of the velocity ratio term. Thus, cavitation studies which use other scale factors are needed to further substantiate the exponent for the diameter ratio. The experimentally determined exponents were $m = 0.5$ and $n = 0.85$. These values are the same as those reported in reference 6. Rewriting equation (5) with the appropriate exponents results in

$$\left(\frac{\forall_v}{\forall_l}\right)_s = \left(\frac{\forall_v}{\forall_l}\right)_f \left(\frac{\alpha_f}{\alpha_s}\right)^{0.5} \left(\frac{D_s}{D_f}\right)^{0.15} \left(\frac{V_{0,s}}{V_{0,f}}\right)^{0.85} \tag{6}$$

From a measured value of Δh_v in a model of given scale, the volume ratio $(\forall_v/\forall_l)_f$ can be determined from figure 13 (or equation (3)). Equation (6) can then be used to de-

termine $(\gamma_v/\gamma_l)_s$ for the liquid, temperature, velocity, and scale of interest. With the new value of $(\gamma_v/\gamma_l)_s$, figure 13 can be used to predict the corresponding value of Δh_v. For the present, equation (6), with the experimentally determined exponents, is offered as the best approach toward generalizing results for different scaled venturis, different liquids and liquid temperatures, and various velocities.

Comparison of Experimental Results with Analysis

A comparison of the experimental data and predicted results for a nominal cavity length of 1.4 diameters is presented in table I. The first line of table I lists the arbitrarily selected test values used as the reference values from which all other tabulated values of Δh_v are predicted. The measured Δh_v selected was 8.5 feet (2.6 m) for 79.9° F (299.8° K) Freon-114 at a velocity of 32.5 feet per second (9.9 m/sec) in the 0.7-scale venturi (fig. 6). The corresponding γ_v/γ_l is 4.6 (from fig. 13). By the use of equation (6) and figure 13, the predicted values of Δh_v of table I were obtained. The Freon-114 and liquid-nitrogen data for the 1.0-scale venturi is from reference 6.

TABLE I. - COMPARISON OF EXPERIMENTAL AND PREDICTED RESULTS FOR A CAVITY LENGTH OF 1.4 FREE-STREAM DIAMETERS

Liquid	Venturi scale	Liquid temperature		Free-stream velocity, V_0		Vapor pressure depression, Δh_v				Vapor - to liquid-volume ratio γ_v/γ_l
						Experimental		Predicted		
		°F	°K	ft/sec	m/sec	ft of liquid	m of liquid	ft of liquid	m of liquid	
Freon-114	0.7	79.9	299.8	32.5	9.9	8.5	2.6	----	---	4.6
		80.1	299.9	44.5	13.6	10.8	3.3	10.6	3.2	6.1
		1.3	256.1	44.0	13.4	.8	.2	.8	.2	5.3
		18.9	265.9	22.1	6.7	.9	.3	.9	.3	3.0
		39.4	277.3	31.1	9.5	2.6	.8	2.5	.8	4.2
Freon-114[a]	1.0	78.8	299.2	31.7	9.7	8.5	2.6	8.6	2.6	4.7
		59.1	288.3	31.7	9.7	5.1	1.6	4.9	1.5	4.6
		78.4	299.0	44.2	13.5	10.2	3.1	10.6	3.2	6.2
Nitrogen[a]	1.0	-320	77.6	20.1	6.1	4.8	1.5	5.6	1.7	2.2
		-320	77.6	25.1	7.7	6.3	1.9	6.6	2.0	2.6

[a]Data from ref. 6.

Good agreement between experimental data and predicted results was observed for all conditions listed in table I. The extended simple theoretical analysis, with the experimentally derived exponents, are useful in predicting cavity pressure depressions for other scaled venturis and liquids, if measured cavity pressure depression data are available for at least one liquid flowing through a geometrically scaled venturi.

Prediction of Free-Stream Static Pressure

As previously presented, $K_{c,\,min}$ for similar cavitation in both the 0.7- and 1.0-scale venturis was approximately the same value (fig. 11). Taking a constant $K_{c,\,min}$ value of 2.44 and using figure 13 to predict trends in cavity pressure depressions, free-stream static pressure h_0 can be estimated for different model scales, liquids, temperatures, and velocities. This is demonstrated by an example. Equation (2a) can be rearranged so that,

$$h_0 = \frac{V_0^2}{2g}(K_{c,\,min}) + h_v - (h_v - h_{c,\,min}) \tag{2b}$$

With the experimental reference data previously used (table I, line 1), h_0 will be estimated for -320° F (77.6° K) nitrogen at a V_0 of 20.1 feet per second (6.1 m/sec) in the 1.0 scale venturi. From equation (6) and figure 13 the predicted Δh_v was 5.6 feet (1.7 m) for this condition (table I, line 9). The value of h_v is 44.2 feet (13.5 m). Therefore, for -320° F (77.6° K) liquid nitrogen at a V_0 of 20.1 feet per second (6.1 m/sec) in the 1.0 scale venturi, the predicted h_0 (eq. (2b)) is 53.9 feet (16.4 m) of liquid. The measured value of h_0 was 54.3 feet (16.6 m) of liquid (ref. 6).

CONCLUDING REMARKS

The method of reference 6 for predicting thermodynamic effects of cavitation in venturis changes in speed, temperature, or liquid was successfully applied to the prediction of pump cavitation performance in reference 2. The method of reference 6 was extended herein to include the effect of scale on the thermodynamic effects of cavitation. It appears likely that this extended prediction method will also be valid for the prediction of pump cavitation performance.

By assuming that the prediction method determined from venturi studies is valid for pumps and inducers, it appears possible to estimate the cavitation performance of full-scale pumps from studies using either geometrically scaled pumps, reduced speeds, or

inexpensive liquids which exhibit thermodynamic effects of cavitation. Any of these methods, or a combination of all three, can mean cost and time reductions in development of large propellant pumps. With experimental reference values obtained in scaled pumps, at reduced speed, or with other liquids, the prediction method can be used to determine the cavitation performance of the full-size pump over a range of operating conditions. However, systematic pump scaling studies are needed to further substantiate these conclusions.

SUMMARY OF RESULTS

Pressure and temperature measurements within well-developed cavitated regions were made of Freon-114 flowing through a 0.7-scale venturi. These results are compared with previously reported results for a 1.0-scale venturi and with theoretical analyses to yield the following principal results:

1. Cavity pressure and temperature depressions for the 0.7-scale venturi were nearly equal to those for the 1.0-scale model for the same free-stream velocity, liquid temperature, and scaled cavity length (same ratio of cavity length to venturi diameter).

2. An available method for predicting the thermodynamic effects of cavitation was extended to account for venturi scale in addition to previous predictable effects of velocity, liquid, and liquid temperature on cavity pressure depressions. This prediction method depends on knowing one measured reference value.

3. Similarity parameters for developed cavitation were evaluated. For the geometrically scaled venturis, a nearly single value was obtained for the cavitation parameter that used the minimum measured cavity pressure as reference. This minimum cavity pressure varied because of the thermodynamic effects of cavitation.

Lewis Research Center,
National Aeronautics and Space Administration,
Cleveland, Ohio, October 5, 1967,
128-31-06-28-22.

APPENDIX

SYMBOLS

c_l	specific heat of liquid, Btu/(lb mass)(^{o}F), (J/(kg)(^{o}K))
C_p	noncavitating pressure coefficient, $(h_x - h_0)/(V_0^2/2g)$
D	free-stream diameter (approach section), in. (cm)
g	acceleration due to gravity, 32.2 ft/sec^2 (9.8 m/sec^2)
h_c	pressure in cavitated region, ft of liquid abs (m of liquid abs)
h_v	vapor pressure corresponding to free-stream liquid temperature, ft of liquid abs (m of liquid abs)
Δh_v	decrease in vapor pressure corresponding to decrease in temperature, ft of liquid (m of liquid)
h_x	static pressure at x, ft of liquid abs (m of liquid abs)
h_0	free-stream static pressure (approach section, fig. 1), ft of liquid abs (m of liquid abs)
J	mechanical equivalent of heat, 778 (ft)-(lb force)/Btu
$K_{c, min}$	developed cavitation parameter based on minimum cavity pressure, $(h_0 - h_{c, min})/(V_0^2/2g)$
K_v	developed cavitation parameter based on free-stream vapor pressure, $(h_0 - h_v)/(V_0^2/2g)$
k	thermal conductivity of saturated liquid, (Btu)/(hr)(ft)(^{o}F), (J/(m)(sec)(^{o}K))
L	latent heat of vaporization, Btu/lb mass (J/kg)
T	free-stream liquid temperature, ^{o}F (^{o}K)
V_0	free-stream velocity (approach section, fig. 1), ft/sec (m/sec)
$\mathscr{V}_l$	volume of saturated liquid, cu ft (cu m)
$\mathscr{V}_v$	volume of saturated vapor, cu ft (cu m)
X	axial distance from venturi inlet (see fig. 1), in. (cm)
x	axial distance from minimum noncavitating pressure location, in. (cm)
Δx	length of cavitated region, in. (cm)
α	thermal diffusivity, $k/\rho_l c_l$, sq ft/hr (sq m/sec)

δ_l thickness of liquid element, in. (cm)

δ_v thickness of vapor cavity, in. (cm)

ρ_l saturated liquid density, lb mass/cu ft (kg/cu m)

ρ_v saturated vapor density, lb mass/cu ft (kg/cu m)

Subscripts:

f full size or reference model

s scale model

min minimum

max maximum

REFERENCES

1. Ball, Calvin L.; Meng, Phillip R.; and Reid, Lonnie: Cavitation Performance of 84° Helical Pump Inducer Operated in 37° and 42° R Liquid Hydrogen. NASA TM X-1360, 1967
2. Ruggeri, Robert S.; Moore, Royce D.; and Gelder, Thomas F.: Method for Predicting Pump Cavitation Performance. Paper presented at the ICRPG Ninth Liquid Propulsion Symposium, St. Louis, Oct. 25-27, 1967.
3. Salemann, Victor: Cavitation and NPSH Requirements of Various Liquids. J. Basic Eng., vol. 81, no. 2, June 1959, pp. 167-180.
4. Spraker, W. A.: The Effects of Fluid Properties on Cavitation in Centrifugal Pumps. J. Eng. Power, vol. 87, no. 3, July 1965, pp. 309-318.
5. Stepanoff, A. J.: Cavitation Properties of Liquids. J. Eng. Power, vol. 86, no. 2, Apr. 1964, pp. 195-200.
6. Gelder, Thomas F.; Ruggeri, Robert S.; and Moore, Royce D.: Cavitation Similarity Considerations Based on Measured Pressure and Temperature Depressions in Cavitated Regions of Freon-114. NASA TN D-3509, 1966.
7. Ruggeri, Robert S.; and Gelder, Thomas F.: Cavitation and Effective Liquid Tension of Nitrogen in a Tunnel Venturi. NASA TN D-2088, 1964.
8. Gelder, Thomas F.; Moore, Royce D.; and Ruggeri, Robert S.: Incipient Cavitation of Freon-114 in a Tunnel Venturi. NASA TN D-2662, 1965.
9. Ruggeri, Robert S.; Moore, Royce D.; and Gelder, Thomas F.: Incipient Cavitation of Ethylene Glycol in a Tunnel Venturi. NASA TN D-2722, 1965.
10. Ruggeri, Robert S.; and Gelder, Thomas F.: Effects of Air Content and Water Purity on Liquid Tension at Incipient Cavitation in Venturi Flow. NASA TN D-1459, 1963.
11. Moore, Royce D.; Ruggeri, Robert S.; and Gelder, Thomas F.: Effects of Wall Pressure Distribution and Liquid Temperature on Incipient Cavitation of Freon-114 and Water in Venturi Flow. NASA Technical Note; estimated publication date, January, 1968.
12. Van Wie; Nelson H.; and Ebel, Robert A.: Some Thermodynamic Properties of Freon-114. Vol. 1. -40° to the Critical Temperature. Rep. No. K-1430, AEC, Sept. 2, 1959.
13. Anon.: "Freon." Bull. No. X-78, Products Div., E. I. DuPont de Nemours and Co., Inc.

NASA-Langley, 1968 —— 12 E-4082

"The aeronautical and space activities of the United States shall be conducted so as to contribute . . . to the expansion of human knowledge of phenomena in the atmosphere and space. The Administration shall provide for the widest practicable and appropriate dissemination of information concerning its activities and the results thereof."

—NATIONAL AERONAUTICS AND SPACE ACT OF 1958

NASA SCIENTIFIC AND TECHNICAL PUBLICATIONS

TECHNICAL REPORTS: Scientific and technical information considered important, complete, and a lasting contribution to existing knowledge.

TECHNICAL NOTES: Information less broad in scope but nevertheless of importance as a contribution to existing knowledge.

TECHNICAL MEMORANDUMS: Information receiving limited distribution because of preliminary data, security classification, or other reasons.

CONTRACTOR REPORTS: Scientific and technical information generated under a NASA contract or grant and considered an important contribution to existing knowledge.

TECHNICAL TRANSLATIONS: Information published in a foreign language considered to merit NASA distribution in English.

SPECIAL PUBLICATIONS: Information derived from or of value to NASA activities. Publications include conference proceedings, monographs, data compilations, handbooks, sourcebooks, and special bibliographies.

TECHNOLOGY UTILIZATION PUBLICATIONS: Information on technology used by NASA that may be of particular interest in commercial and other non-aerospace applications. Publications include Tech Briefs, Technology Utilization Reports and Notes, and Technology Surveys.

Details on the availability of these publications may be obtained from:

SCIENTIFIC AND TECHNICAL INFORMATION DIVISION

NATIONAL AERONAUTICS AND SPACE ADMINISTRATION

Washington, D.C. 20546